Insights into Photodissociation Dynamics of Propionyl Chloride from ab Initio Calculations and Molecular Dynamics Simulations

Shi-Lv Chen and Wei-Hai Fang*

Department of Chemistry, Beijing Normal University, Beijing 100875, P. R. China

Received: August 22, 2005

The potential energy surfaces of isomerization, dissociation, and elimination reactions for CH_3CH_2COCl in the S_0 and S_1 states have been mapped with the different ab inito calculations. Mechanistic photodissociation of CH_3CH_2COCl at 266 nm has been characterized through the computed potential energy surfaces, the optimized surface crossing structure, intrinsic reaction coordinate, and ab initio molecular dynamics calculations. Photoexcitation at 266 nm leads to the CH_3CH_2COCl molecules in the S_1 state. From this state, the C−Cl bond cleavage proceeds in a time scale of picosecond in the gas phase. The barrier to the C−Cl bond cleavage on the S_1 surface is significantly increased by effects of the matrix and the internal conversion to the ground state prevails in the condensed phase. The HCl eliminations as a result of internal conversion to the ground state become the dominant channel upon photodissociation of CH_3CH_2COCl in the argon matrix at 10 K.

Introduction

Propionyl chloride (CH_3CH_2COCl) is an important organic compound, and particular attention has been recently devoted to its photodissociation.[1−3] The photodissociation of CH_3CH_2COCl is interesting from both an environmental and fundamental chemistry perspective.[4,5] The discharge of chlorine-containing compounds into the environment has raised concern regarding their potential impact on stratospheric ozone abundances and groundwater supplies. In saturated carbonyl compounds, the dominant dissociation pathway upon photoexcitation is cleavage of a bond α to the carbonyl group, the Norrish type I reaction, which is characteristic of asymmetrically substituted aldehydes and ketones. However, CH_3CH_2COCl appears not to follow the Norrish type I reaction,[1−3] although it is a representative of asymmetrically substituted carbonyl compounds. In addition, the propionyl radical plays a significant role in combustion processes and atmospheric chemistry;[1,4,6] it can be generated by cleaving the C−Cl bond of CH_3CH_2COCl.

Early studies have been carried out on equilibrium structures of CH_3CH_2COCl in the gas phase.[7−10] It was found that CH_3CH_2COCl in the ground state exists as a mixture of two conformers, the *s*-trans and the gauche rotamers, with the *s*-trans conformer being the more stable form. Karlsson[7] and Mata et al.[8] from microwave studies predicted the barrier to rotation of the methyl group of the *s*-trans conformer to be at ∼870 cm^{-1} (2.5 kcal/mol). Evidence for existence of both the *s*-trans and gauche conformers was found from the electron diffraction study,[10] and the dihedral angle in the gauche conformer was estimated at 113−127°. The energy difference between the two conformers was found to be 1−2 kcal/mol.[9,10] The far-infrared spectrum of gaseous propionyl chloride has been recorded at a resolution of 0.10 cm^{-1}, and a substantial number of bands have been assigned to both the symmetric and asymmetric torsional modes,[11] which provide values of about 2.2, 2.9, and 0.8 kcal/mol for the *s*-trans to gauche, gauche to gauche, and gauche to *s*-trans barriers, respectively.

To understand the mechanism for the condensed-phase photodecomposition of the acid chlorides, Winter and coworkers[2] have used FTIR absorption spectroscopy to probe the photodecomposition products of propionyl chloride in an Ar matrix at 10 K following irradiation at 248, 254, and 266 nm. The observed products are methyl ketene (CH_3CHCO) and hydrochloric acid (HCl) by α-elimination.

$$CH_3CH_2COCl + h\nu \rightarrow CH_3CHCO + HCl \qquad (1)$$

No other products were detected even after prolonged irradiation of CH_3CH_2COCl. It was suggested that the reaction does not proceed via hydrogen abstraction by a free chlorine atom but rather through a direct elimination process. Photofragment translational spectroscopy was used to study the photodissociation of CH_3CH_2COCl at 248 nm.[3] The crossed laser−molecular beam experiment with VUV photoionization showed two primary dissociation channels, the HCl elimination and C−Cl bond fission,

$$CH_3CH_2COCl + h\nu \rightarrow CH_3CH_2CO + Cl \qquad (2)$$

The HCl elimination was observed as the minor primary dissociation in the gas phase, which could occur by *β*-elimination,

$$CH_3CH_2COCl + h\nu \rightarrow CH_2CH_2CO + HCl \qquad (3)$$

The formed CH_2CH_2CO radical undergoes secondary dissociation to produce CO and $CH_2{=}CH_2$ with a significant amount of energy partitioned into translational motion.[3] To explore dissociation behavior of the propionyl radical, photolysis of gaseous CH_3CH_2COCl at 248 nm has been studied by time-resolved Fourier transform infrared spectroscopy.[1]

Although there are several experimental studies regarding photodissoiation of CH_3CH_2COCl in the gas and condensed phases, the inferences about the reaction mechanisms are rather speculative and not well-substantiated in these studies. The C−C and C−Cl bonds have similar strength; however, the only products from the C−Cl bond cleavage were observed upon photodissociation of gaseous CH_3CH_2COCl at a wavelength

* Corresponding author. Tel.: +86-10-58805382. Fax: +86-10-5880-2075. E-mail: fangwh@bnu.edu.cn.

10.1021/jp0547257 CCC: $33.50
Published on Web 12/16/2005

range of 248−266 nm. It has been found that CH_3CH_2COCl photodissociates to form exclusively CH_3CHCO and HCl in the condensed phase following excitation at 248 nm. However, the HCl elimination was observed as the minor primary dissociation in the gas phase. Analogous dependence of photoproducts on the initial phase of the reactant was found for acetyl chloride (CH_3COCl).[12,13] As far as we know, there are only three ab initio studies[2,11,14] on structure and properties of CH_3CH_2COCl in the ground state. As a complementary of experimental work, structural parameters, fundamental vibrational frequencies, and relative energies of the *s*-trans and gauche isomers were determined from ab initio Hartree−Fock calculations employing the 3-21G* and 6-31G* basis sets.[11] The B3LYP/cc-pVDZ and MP2/6-311G* electronic structure calculations[2,14] were carried out to determine the ground-state geometries and to identify the harmonic frequencies of CH_3CH_2COCl and CH_3CHCO.

To provide new insights into the photodissociation mechanism of acid chlorides, we took CH_3CH_2COCl as a representative in the present work and have carried out density functional theory (DFT) and complete-active-space self-consistent field (CASSCF) studies on potential energy profiles of the CH_3CH_2COCl dissociation and isomerization in the ground (S_0) and first excited singlet (S_1) states. Ab initio molecular dynamics calculations were conducted to determine the initial relaxation process from the S_1 Franck−Condon geometry and the HCl elimination dynamics. The S_1 C−Cl bond cleavage is predicted to occur in about 200 fs and is the dominant primary process upon photodissociaiton of CH_3CH_2COCl in the gas phase. The β-elimination of HCl in the ground state is confirmed to be a synchronous concerted three-body dissociation process,

$$CH_3CH_2COCl + h\nu \rightarrow CH_2{=}CH_2 + CO + HCl \quad (4)$$

The barrier to the C−Cl bond cleavage on the S_1 surface is significantly increased by effects of the matrix, and the internal conversion to the ground state prevails. The HCl eliminations become the dominant channel upon photodissociation of CH_3CH_2COCl in the argon matrix at 10 K.

Computational Methods

Stationary structures on the S_0 potential energy surface (PES) have been optimized with the B3LYP method, which is composed of Becke's three-parameter hybrid exchange functional (B3)[15] and the correlation functional of Lee, Yang, and Parr (LYP).[16] The harmonic vibrational frequencies were examined to confirm the optimized structure to be a true minimum or first-order saddle point on the S_0 PES. The IRC (intrinsic reaction coordinate) calculations have been carried out at the B3LYP level with the saddle-point structures as the starting points to confirm the optimized saddle point to be on the correct reaction pathway. The complete-active-space self-consistent field (CASSCF) wave function has sufficient flexibility to model the changes in electronic structure upon electronic excitation,[17] which is employed to optimize stationary structures on the S_1 potential energy surface of the C−Cl and C−C bond fissions. The state-averaged (SA) CASSCF method[18] was used to determine geometry on the intersection space of two different electronic states. In the CASSCF calculations, the active space is composed of eight electrons distributed in seven orbitals, referred to as CAS(8,7) hereafter. The CAS(8,7) calculation is related to limited inclusion of electron correlation effect. To compensate for this, the single-point energy is calculated with the MR-CI method on the CAS(12,10) wave functions. The cc-pVDZ and cc-pVTZ basis sets[19] are used in the present study. The CASSCF and DFT calculations were performed using the Gaussian 98 and 03 packages of programs,[20] while the MOLPRO program package[21] was used to perform the MR-CI calculations.

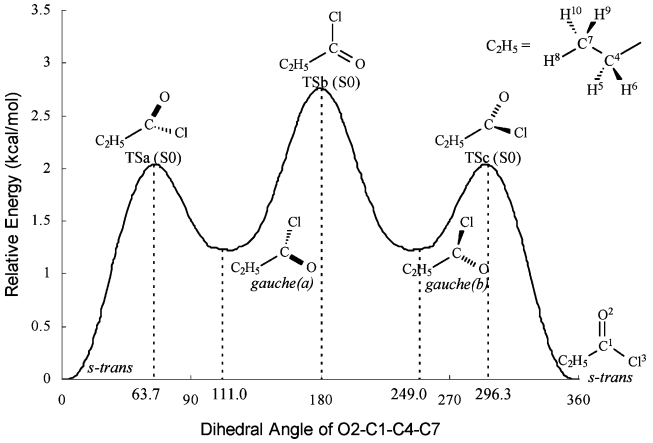

Figure 1. Schematic potential energy surface for the rotational isomerization of CH_3CH_2COCl in the ground state, along with the stationary structures and their relative energies (kcal/mol).

Ab initio classical trajectory calculations[22,23] were performed using a Born−Oppenheimer molecular dynamics model[24,25] with a step size of 0.25 amu$^{1/2}$ bohr. The trajectories were started at the transition state of the three-body dissociation and were stopped when the centers of mass of the products were 12 bohrs apart. Fifty trajectories were integrated at the B3LYP/cc-pVDZ level for the three-body dissociation of CH_3CH_2COCl in the ground state. The initial conditions for the trajectory calculations were chosen to simulate photolysis of CH_3CH_2COCl at 248 nm.

Results and Discussion

Isomerization Reactions. Experimentally, it has been found that CH_3CH_2COCl in the ground state exists as a mixture of two conformers,[7−11] which are labeled by *s-trans*-CH_3CH_2COCl and *gauche(a)*-CH_3CH_2COCl in Figure 1. The third rotational isomer is predicted to be a stable conformer by the B3LYP/cc-pVDZ calculations, referred to as *gauche(b)*-CH_3CH_2COCl hereafter. The optimized structures are schematically shown in Figure 1 along with the atomic numbers in the *s-trans*-CH_3CH_2COCl structure. The B3LYP/cc-pVDZ bond parameters for the three isomers are given in Supporting Information. All of the heavy atoms are in the plane of symmetry in the *s-trans*-CH_3CH_2COCl structure. The bond parameters of the ethyl moiety are nearly unchanged from *s-trans*-CH_3CH_2COCl to *gauche*(*a*)-CH_3CH_2COCl and to *gauche*(*b*)-CH_3CH_2COCl. The striking change in structure is associated with the O2−C1−C4−C7 dihedral angle, which is 0.0° in *s-trans*-CH_3CH_2COCl and becomes 111.0° and −111.0° in *gauche*(*a*)- and *gauche*(*b*)-CH_3CH_2COCl, respectively. The dihedral angle of the gauche conformer was inferred to be 108.5 ± 0.5° experimentally.[11] Structural difference of the three isomers arises from the relative orientation of the ClCO group with respect to the ethyl moiety. The *s-trans*-CH_3CH_2COCl isomer is the most stable with the same relative energy of 1.2 kcal/mol for *gauche*(*a*)- and *gauche*(*b*)-CH_3CH_2COCl at the B3LYP/cc-pVDZ level. The energy difference between *s-trans*- and *gauche*-CH_3CH_2COCl was determined to be 491 ± 81 cm^{-1} (1.2−1.6 kcal/mol) by the variable-temperature study of the Raman spectrum of propionyl chloride in the gas phase,[11] which is close to the corresponding value of 502 ± 167 cm^{-1} from the electron diffraction data.[10]

Three transition states were found in the ground state, which are labeled, respectively, with TSa(S_0), TSb(S_0), and TSc(S_0). Their structures are depicted in Figure 1. The IRC calculations at the B3LYP/cc-pVDZ level clearly show that TSa(S_0), TSb(S_0), and TSc(S_0) are the transition states to connect s-trans and gauche(*a*), gauche(*a*) and gauche(*b*), and gauche(*b*) and s-trans isomers, respectively. On the basis of the IRC calculated energies, the potential energy profiles are plotted in Figure 1, which can be regarded as a function of the dihedral angle of O2−C1−C4−C7. The energy barriers to the rotational isomerization from s-trans to gauche(*a*), from gauche(*a*) to gauche(*b*,) and from gauche(*b*) to *s*-trans conformers are predicted to be 2.0, 1.5, and 0.8 kcal/mol, respectively, by the B3LYP/cc-pVDZ calculations. The corresponding values were experimentally inferred to be 2.2, 2.9, and 0.8 kcal/mol.[11] The bond parameters and relative energies obtained by the B3LYP/cc-pVTZ calculations are very close to those from the B3LYP/cc-pVDZ calculations and are in excellent agreement with the experimental findings where available. It is obvious that the present B3LYP calculations provide a good description of the structures and energies of CH_3CH_2COCl in the ground state.

α-Elimination of HCl. The dissociation of CH_3CH_2COCl into CH_3CHCO + HCl is an α-elimination process. A transition state was optimized at the B3LYP/cc-pVDZ level and confirmed to be the first-order saddle point on the S_0 pathway, which is denoted by $TS1_{HCl}(S_0)$. Its structure is shown in Figure 2. The C1−Cl3 and H5−Cl3 distances are, respectively, 2.882 and 1.848 Å in the $TS1_{HCl}(S_0)$ structure. The large C1−Cl3 separation gives us a hint that $TS1_{HCl}(S_0)$ could be a transition state for hydrogen abstraction of the propionyl radical by the free chlorine atom. To confirm $TS1_{HCl}(S_0)$ to be the transition state of the direct HCl elimination, the IRC calculations were carried out at the B3LYP/cc-pVDZ level with the $TS1_{HCl}(S_0)$ structure as the starting point. $TS1_{HCl}(S_0)$ was confirmed to connect the *gauche(a)*-CH_3CH_2COCl on the reactant side and CH_3CHCO + HCl on the product side. The IRC energies are plotted in Figure 3 as a function of reaction coordinate. The direct α-elimination of HCl has a barrier of 43.1 kcal/mol at the B3LYP/cc-pVDZ level and 43.4 kcal/mol at the B3LYP/cc-pVTZ level. The barrier becomes 39.6 and 39.5 kcal/mol with the zero-point energy correction included at the B3LYP/cc-pVDZ and B3LYP/cc-pVTZ levels, respectively.

All attempts to optimize a transition state for the direct α-elimination of HCl on the S_1 state were unsuccessful. The direct α-elimination of HCl involves cleavages of the C−Cl and C−H bonds, formation of the H−Cl bond, and a large deformation of the molecular structure, simultaneously. It is reasonable to expect that on the S_1 state the direct α-elimination should not compete with the C−Cl bond fission and other photophysical processes. Methyl ketene ($CH_3CH{=}C{=}O$) and HCl were observed as exclusive products upon photodissociation of CH_3CH_2COCl in the argon matrix at 10 K.[2] The α-elimination of HCl was proposed to proceed directly along the S_0 pathway as a result of internal conversion from an excited singlet state. Both the present theoretical calculations and the previous experimental observation agree in predicting that the direct α-elimination of HCl occurs on the S_0 surface.

***β*-Elimination of HCl.** The distance between the Cl3 atom and the methyl H9 atom is 4.516 Å in *s-trans*-CH_3CH_2COCl at the B3LYP/cc-pVDZ level, but this distance is 2.925 Å in *gauche*(*a*)-CH_3CH_2COCl at the same level of theory. The calculated Cl3−H9 distance gives us a hint that the *β*-elimination of HCl maybe starts from the *gauche*(*a*)-CH_3CH_2COCl isomer in the ground state. A transition state was optimized at the B3LYP/cc-pVDZ level and was confirmed to be the first-order saddle point on the S_0 surface, which is referred to as $TS2_{HCl}(S_0)$ hereafter. The optimized $TS2_{HCl}(S_0)$ structure is schematically depicted in Figure 2, along with the key bond parameters from the B3LYP/cc-pVDZ calculations. The Cl3−C1 and C4−C1 bonds are nearly broken in $TS2_{HCl}(S_0)$ with the Cl3−C1 and C4−C1 distances of 2.533 and 2.230 Å, respectively. In addition, the C4 − C7 bond is partially of double bond character in the $TS2_{HCl}(S_0)$ structure. The optimized structure shows that $TS2_{HCl}(S_0)$ is probably the transition state of the *gauche*(*a*)-CH_3CH_2COCl three-body dissociation to CH_2-CH_2 + CO + HCl. This was first confirmed by the IRC calculations with the $TS2_{HCl}(S_0)$ structure as the starting point. Figure 3 shows the potential energy profile along the mass-weighted steepest descent reaction pathway, which comes from the IRC calculations at the B3LYP/cc-pVDZ level. The B3LYP/cc-pVDZ calculations provide a barrier of 61.1 kcal/mol for the synchronous concerted three-body dissociation of CH_3CH_2-

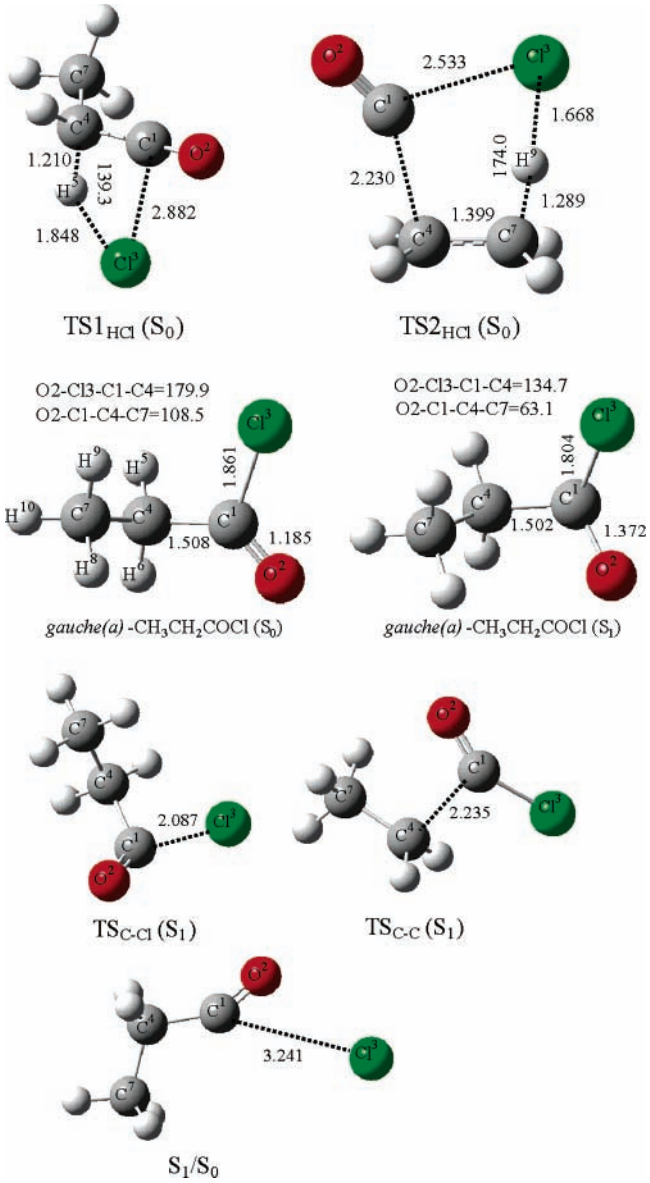

Figure 2. The stationary and intersection structures along with the selected CAS(8,7)/cc-pVDZ bond parameters for *gauche*(*a*)-$CH_3CH_2COCl(S_0)$, *gauche*(*a*)-$CH_3CH_2COCl(S_1)$, $TS_{C-Cl}(S_1)$, $TS_{C-C}(S_1)$, and S_1/S_0, and the B3LYP/cc-pVDZ bond parameters for $TS1_{HCl}(S_0)$ and $TS2_{HCl}(S_0)$ (bond lengths in Å, and bond angles and dihedral angles in degrees).

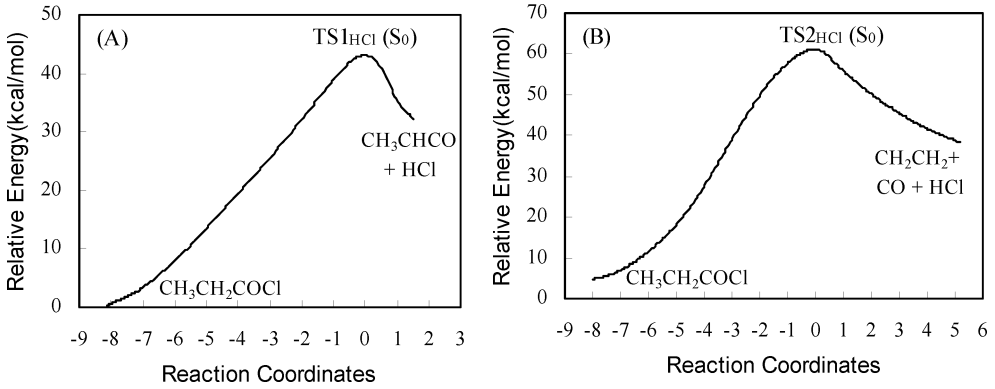

Figure 3. Schematic potential energy surfaces of the HCl elimination reactions, $CH_3CH_2COCl \rightarrow CH_3CHCO + HCl$ (A) and $CH_3CH_2COCl \rightarrow CH_2CH_2 + CO + HCl$ (B).

COCl into $CH_2CH_2 + CO + HCl$. The same barrier height was obtained by the B3LYP calculations with the cc-pVTZ basis set. The barrier height is reduced to 55.5 kcal/mol when the zero-point energy correction is considered. Like the direct α-elimination of HCl, the *β*-elimination of HCl occurs on the ground state. There is little probability that the direct *β*-elimination of HCl proceeds along the S_1 pathway.

The IRC calculations ignore the effects of vibrational and kinetic energies on the reaction processes. It has been shown that reactions do not necessarily follow the IRC pathways when kinetic energy is accounted for.[26,27] In addition, three-body dissociations are of fundamental significance in physical chemistry and much importance in atmospheric and combustion processes, and there exist only a few studies[28,29] for photoinduced three-body reactions with three molecules as products. In view of these, the three-body dissociation of CH_3CH_2COCl to $CH_2CH_2 + CO + HCl$ has been studied by direct classical trajectory calculations using the B3LYP/cc-pVDZ method. The initial conditions for the trajectory calculations were chosen to simulate photolysis of CH_3CH_2COCl at 248 nm with the initial kinetic energy of 59.8 kcal/mol, which corresponds to the energy difference between the 248-nm photon (115.3 kcal/mol) and the $TS2_{HCl}(S_0)$ energy (55.5 kcal/mol). The distances between the centers of mass are plotted in Figure 4 as a function of time for all fifty trajectories. The trajectories start from the $TS2_{HCl}(S_0)$ structure, and the distances between the centers of mass for any pair of fragments (CO, HCl, and C_2H_4) are larger than 12 bohrs after 200-fs propagations of the trajectories. This gives further evidence that the *β*-elimination of HCl from CH_3CH_2COCl is a synchronously concerted three-body process with CO and CH_2CH_2 as coproducts.

The HCl elimination was reported as the minor primary dissociation channel upon photoexcitation of CH_3CH_2COCl in the gas phase, and the reaction could occur by the *β*-elimination.[3] The CO and $CH_2{=}CH_2$ were observed as coproducts with a significant amount of translational energies. However, the *β*-elimination of HCl was proposed via a two-step process: $CH_3CH_2COCl \rightarrow CH_2CH_2CO + HCl$ and $CH_2CH_2CO \rightarrow CH_2CH_2 + CO$. This mechanism is not supported by the present IRC and classical trajectory calculations, which predict the *β*-elimination of HCl from CH_3CH_2COCl to be a synchronously concerted three-body process.

α-C−Cl and α-C−C Bond Cleavages. Photoexcitation of a carbonyl compound from the ground state (S_0) to its first excited state (S_1) leads primarily to the cleavage of a bond α to the carbonyl group, which is referred to as a Norrish type I reaction. There are comparable pre-exponential factors for different bond fissions, and the relative strengths of the α-bonds closely approximate the relative barrier heights. It is generally thought that the weaker of the two α-bonds cleaves most readily upon low-energy photon excitation. However, experimental investigations[1−3] on photodissociation of CH_3CH_2COCl have demonstrated that the α-C−Cl bond breaks in high yield and cleavage of the α-C−C bond occurs with little probability, although the two α-bonds have similar strength. The underlying reason remains unclear to date. Here, the potential energy surfaces of the α-C−Cl and α-C−C bond cleavages were determined by the combined MR-CI/CASSCF calculations.

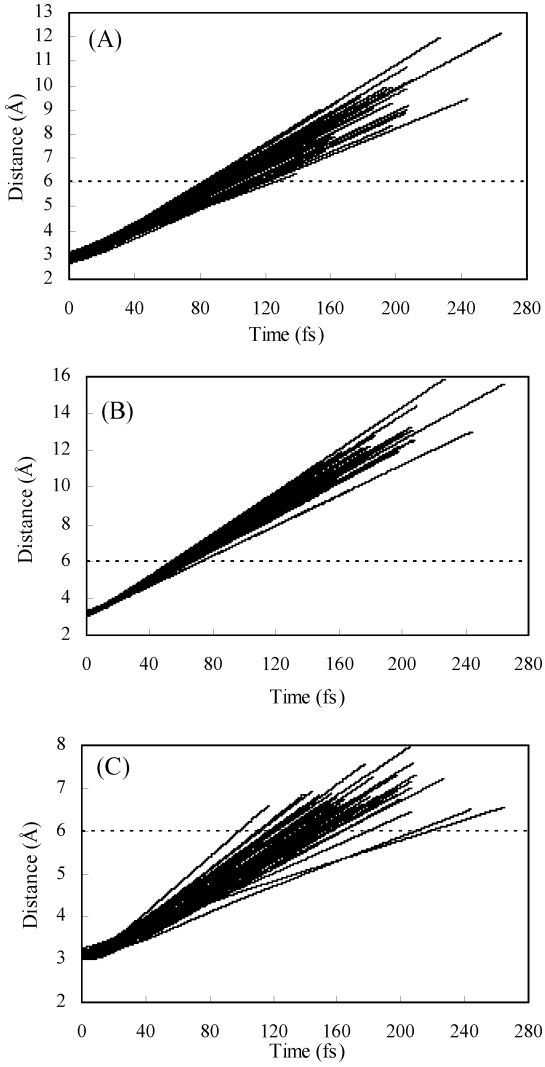

Figure 4. The distances among the CO, HCl, and C_2H_4 centers of mass are plotted as functions of time for the fifty trajectories starting from the transition state of $TS2_{HCl}(S_0)$ for the *β*-elimination of HCl. (A) CO and HCl; (B) CO and C_2H_4; (C) HCl and C_2H_4.

Both ClCO and CH_3CH_2 radicals have $^2A'$ symmetry in the ground state. When the two ground-state radicals approach each other in C_1 symmetry, they can correlate with CH_3CH_2COCl in the S_0 state. Therefore, the CH_3CH_2COCl in the S_1 state only can correlate with the $ClCO(^2A'')$ and $CH_3CH_2(^2A')$ fragments in an excited state. Unlike the α-C−C bond cleavage, fission of the α-C−Cl bond produces the Cl atom as one of the fragments. The Cl atom has ^2P species, which is 3-fold degenerate. When the $Cl(^2P)$ atom and the $CH_3CH_2CO(\tilde{X}^2A')$ radical approach each other in C_1 symmetry, they can correlate adiabatically with the S_0, S_1, and S_2 states of CH_3CH_2COCl. The qualitative state correlation analysis is consistent with the calculated potential energy surfaces of α-C−Cl and α-C−C bond cleavages, which will be discussed below.

CH_3CH_2COCl may dissociate into $CH_3CH_2CO + Cl$ and $CH_3CH_2 + ClCO$ along the ground-state pathways. We have made efforts to optimize a transition state for the α-C−Cl or α-C−C bond cleavage in the ground state, but optimizations always lead to the dissociation limit of $CH_3CH_2CO + Cl$ or $CH_3CH_2 + ClCO$. It is evident that no potential barrier above endothermicity exists on the S_0 pathway to $CH_3CH_2CO + Cl$ or $CH_3CH_2 + ClCO$. The α-C−Cl and α-C−C bond cleavages of CH_3CH_2COCl are, respectively, endothermic by 83.1 and 85.7 kcal/mol estimated from heats of formation at 0 K.[2]

The S_1 equilibrium geometry of CH_3CH_2COCl is optimized with the CAS(8,7)/cc-pVDZ approach. The resulting structure is shown in Figure 2, along with the key CAS(8,7)/cc-pVDZ bond parameters. In comparison with the equilibrium geometry in the ground state, the C−O bond length is elongated by 0.187 Å in the S_1 structure. The O2−Cl3−C1−C4 dihedral angle is decreased from 180.0° in the S_0 structure to 134.7° in the S_1 structure. Natural orbital analysis clearly shows that the S_1 state originates from the n → π* excitation. One-electron excitation from the n to the π* orbital leads to a partial breaking of the C═O π-bond. As a result of this, the C−O bond is significantly elongated in S_1 with respect to that in S_0. From the viewpoint of valence bond theory, the n → π* excitation makes the carbonyl C atom rehybridize from sp^2 in the ground state to sp^3 in the S_1 state, resulting in the S_1 pyramidal structure at the carbonyl carbon atom. In fact, the S_1 state has common pyramidal equilibrium geometry for a wide variety of aliphatic carbonyl molecules.[30−33]

The adiabatic excitation energy (0−0 energy gap) from S_0 to S_1 was first calculated with the CAS(8,7)/cc-pVDZ approach, which gives the value of 104.7 kcal/mol for the $S_0 \rightarrow S_1$ transition of CH_3CH_2COCl. On the basis of the CAS(8,7)/cc-pVDZ optimized structures for the S_0 and S_1 states, the 0−0 energy gap was predicted to be 95.4 kcal/mol by the MR-CI single-point energy calculations. As far as we know, the band origin for the $S_0 \rightarrow S_1$ transition of CH_3CH_2COCl has not been reported in the literature to date. Two transition states, referred to as $TS_{C-C}(S_1)$ and $TS_{C-Cl}(S_1)$ in Figure 2, were found on the S_1 surface and confirmed to be the first-order saddle points by frequency calculations. The imaginary vibrational modes show that $TS_{C-C}(S_1)$ and $TS_{C-Cl}(S_1)$ are the transition states on the S_1 pathways to $CH_3CH_2(\tilde{X}^2A') + COCl(\tilde{A}^2A)$ and $CH_3CH_2CO(\tilde{X}^2A') + Cl(^2P)$, respectively. At the CAS(8,7)/cc-pVDZ level, the C−C distance is 2.235 Å in $TS_{C-C}(S_1)$ and the C−Cl distance is 2.087 Å in $TS_{C-Cl}(S_1)$, which are 0.733 and 0.283 Å longer than the corresponding values in the S_1 minimum. With respect to the vibrational zero-level of the S_1 state, the barrier heights for the C−C and C−Cl bond fissions on the S_1 surface are 43.3 and 4.4 kcal/mol at the CAS(8,7)/cc-pVDZ level, respectively. They become 30.8 and 1.0 kcal/mol by the MR-CI single-point energy calculations. The potential energy surfaces for the C−C and C−Cl bond cleavages are shown in Figure 5, along with the MR-CI relative energies of the optimized stationary structures. It is obvious that the S_1 barrier to the α-C−Cl bond cleavage is much lower than that for the α-C−C bond fission along the S_1 pathway. As discussed before, the S_1 C−C bond fission leads to the $CH_3CH_2(\tilde{X}^2A') + COCl(\tilde{A}^2A)$ fragments in the excited state with high endothermicity, while the S_1 C−Cl bond cleavage produces the $CH_3CH_2CO(\tilde{X}^2A') + Cl(^2P)$ fragments in the ground state and is exothermic by about 12 kcal/mol. These are the main reasons why the S_1 C−C bond fission has a barrier that is much higher than that for the S_1 C−Cl bond cleavage, which provides a reasonable explanation of why the C−Cl bond cleavage was experimentally observed to be the dominant channel upon n → π* excitation of CH_3CH_2COCl.

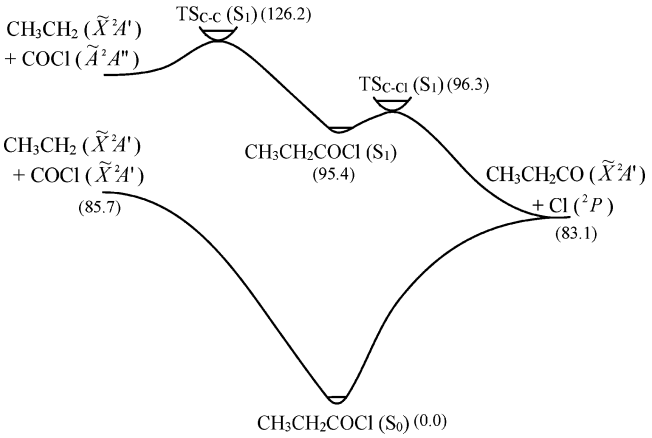

Figure 5. Schematic potential energy profiles for the C−C and C−Cl bond cleavages of CH_3CH_2COCl in the S_0 and S_1 states, along with the MR-CI relative energy (kcal/mol).

Dynamics of the S_1 C−Cl Cleavage. On the basis of the CAS(8,7)/cc-pVDZ frequencies and MR-CI energies for the S_1 minimum and $TS_{C-Cl}(S_1)$ structures, the adiabatic RRKM theory of rate[34,35] is employed to calculate the rate constant of the α-C−Cl bond cleavage along the S_1 pathway. Since rotational degrees of freedom have less effect on the RRKM rate constant, only vibrational degrees of freedom are considered with a harmonic approximation. The RRKM rate constant is computed to be 7.3×10^{12} s^{-1} for the S_1 α-C−Cl bond cleavage with a total angular momentum of $J = 0$ and a total energy of $E = 19.9$ kcal/mol, which corresponds to the energy difference between the 248-nm photon and the S_1 vibrational zero level. The calculated rate constant for the S_1 α-C−Cl bond cleavage is very close to the limit where energy flows rapidly and randomly among all the vibrational degrees of freedom, which is the premise for the RRKM rate calculations. It is a question if the rate constant calculated with the statistical RRKM theory is reliable for the present case. To clarify this question, we performed ab initio molecular dynamic calculations on the Born−Oppenheimer surface.[25]

The initial conditions for trajectory calculations have been chosen to simulate the experimental photodissociation of CH_3CH_2COCl at 248 nm. The trajectory is started from the S_1 FC geometry with 5.0 kcal/mol as the initial kinetic energy, which is randomly distributed among the vibrational degrees of freedom. The potential energy and the key bond parameters as a function of time are plotted in Figure 6. The C−Cl bond length is decreased to the S_1 equilibrium at the initial stage, and then the C−Cl bond cleaves after 140 fs. The C−O bond length is 1.185 Å at the starting point of the trajectory, and it increases

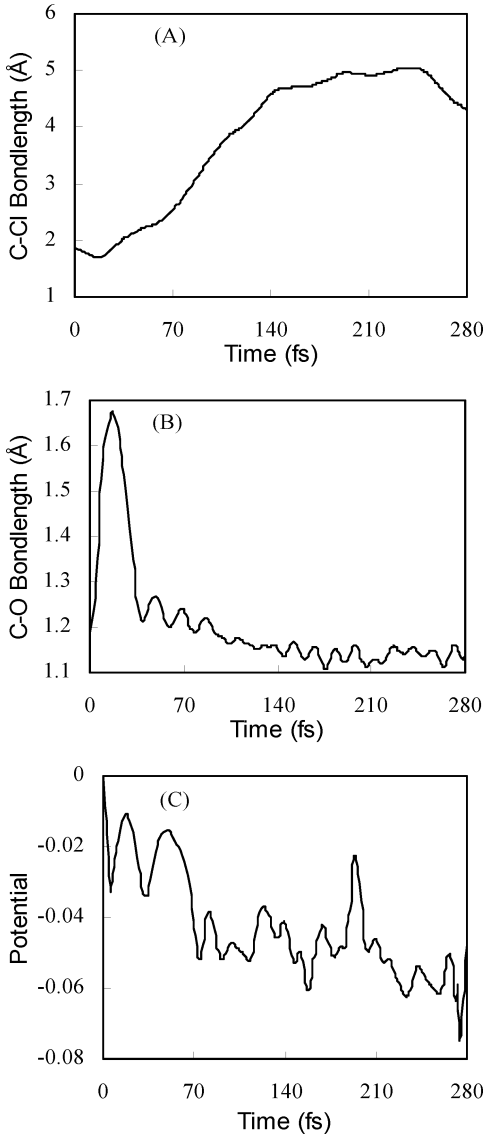

Figure 6. The C−Cl distance (A), the C−O distance (B), and the CASSCF energies (C) are plotted as functions of time for the trajectory starting from the S_1 Franck−Condon geometry.

very fast to a maximum value of 1.678 Å. After 140-fs propagation, the C−O bond length oscillates in the vicinity of 1.15 Å. Similarly, the O2−Cl3−C1−C4 dihedral angle is changed from 180.0° at the S_1 FC structure to about 130° in the vicinity of the S_1 minimum and to about 90° in the fragment region. The corresponding changes in energy can be seen from Figure 6. On average, the trajectory reaches the $TS_{C-Cl}(S_1)$ region after 70-fs propagation and mainly moves about in the fragment region after 140 fs. Ab initio molecular dynamics calculations predict that the S_1 α-C−Cl bond cleavage occurs within 200 fs, which corresponds to a rate constant of 5×10^{12} s^{-1}. This is close to that from the RRKM rate calculations.

Mechanistic Aspects. Photoexcitation at 266 nm leads to the CH_3CH_2COCl molecules in the S_1 state. From this state, the CH_3CH_2COCl molecules can deactivate via three nonradiative channels. They are internal conversion (IC) to the ground state, intersystem crossing (ISC) to the T_1 state, and the direct dissociations along the S_1 pathways. As pointed out before, the α-C−C bond fission has a barrier of 30.8 kcal/mol (126.2 kcal/mol above the S_0 vibrational zero level) on the S_1 pathway. Therefore, the S_1 fission of the α-C−C bond is energetically inaccessible upon photoexcitation at 266 nm (107.3 kcal/mol). Since the HCl elimination involves breakage and formation of a few bonds simultaneously, the α- or β-elimination of HCl is not in competition with the α-C−Cl bond cleavage on the S_1 surface. It is reasonable to exclude probabilities that the α-C−C bond fission and α- and β-eliminations of HCl proceed along the S_1 pathways. The C−Cl bond fission was experimentally observed to be the dominant channel in the gas phase,[1,3] which is in good agreement with the theoretical findings reported here.

The HCl elimination was detected to be an exclusive channel for the CH_3CH_2COCl photodecomposition in the Ar matrix at 10 K.[2] The PCM model[36] was used to simulate the effect of the argon matrix on the C−Cl bond cleavage along the S_1 pathway. The S_1 equilibrium geometry and the $TS_{C-Cl}(S_1)$ structure in the Ar matrix at 10 K were optimized at the CAS(8,7)/cc-pVDZ level. The matrix has little influence on the S_1 equilibrium geometry, but the C−Cl distance is decreased by 0.03 Å in the $TS_{C-Cl}(S_1)$ structure from the gas phase to the Ar matrix at 10 K. The barrier to the S_1 C−Cl bond fission is significantly increased from the gas phase to the argon matrix. Structural relaxation results in an increase of the barrier height by 5.4 kcal/mol, which is obtained by MR-CI calculations on the CAS-(8,7) optimized S_1 and $TS_{C-Cl}(S_1)$ structures in the gas phase and in the matrix without including any other matrix effect. The effect of matrix polarization interaction on the barrier height is estimated by the CAS(8,7) calculated relative energies in the gas phase and in the matrix at the fixed structures. The barrier to the C−Cl bond fission on the S_1 pathway is increased by 5.2 kcal/mol, because of polarization interaction between the system and the matrix. As a result of these, the internal conversion from S_1 to S_0 becomes the dominant process for the CH_3CH_2-$COCl(S_1)$ molecule to deactivate in the condensed phase. Once the "hot" ground-state CH_3CH_2COCl molecules are formed, the α- and β-eliminations of HCl may take place along the S_0 pathways. Since rotation and deformation are restricted in the condensed phase, the β-elimination is blocked by the matrix effect. Therefore, the internal conversion from the S_1 state followed by the α-elimination in the ground state is the most probable mechanism for formation of HCl in the argon matrix at 10 K.

The CAS(8,7)/cc-pVDZ calculations show that in the isolated CH_3CH_2COCl molecule the S_0 and S_1 states are degenerate when the C−Cl separation is larger than 3.241 Å. This C−Cl separation was estimated to be smaller in the argon matrix. Before the C−Cl bond is completely broken along the S_1 pathway, the CH_3CH_2COCl molecule can be reformed in the ground state. In this case, the CH_3CH_2COCl molecules in the S_0 state have sufficient internal energy to overcome the barrier on the pathway of the HCl elimination. This is the minor channel that is responsible for formation of HCl in the gas phase.

Summary

The potential energy surfaces of isomerization, dissociation, and elimination reactions for CH_3CH_2COCl in the S_0 and S_1 states have been mapped with DFT, CASSCF, and MR-CI calculations. Mechanistic photodissociation of CH_3CH_2COCl at 266 nm has been characterized through the computed potential energy surfaces, the optimized surface crossing structure, intrinsic reaction coordinate, and ab initio molecular dynamics calculations. In the gas phase, the S_1 α-C−Cl bond cleavage is the dominant channel upon photoexcitation of CH_3CH_2COCl at 266 nm. Meanwhile, there is a little probability that the system returns to the ground state at a large C−Cl separation, which is followed by the α- and β-eliminations of HCl along the S_0 pathways. This mechanism is consistent with the experimental

findings. The β-elimination is predicted to be a synchronously concerted three-body process, which is different from the two-step elimination mechanism proposed in the previous experimental studies.

The barrier to the C−Cl bond cleavage on the S_1 surface is significantly increased by effects of the matrix. As a result, the internal conversion from S_1 to S_0 becomes the dominant process for the $CH_3CH_2COCl(S_1)$ molecule to deactivate in the condensed phase, which is followed by the HCl eliminations in the ground state. This is the main pathway that is responsible for the HCl eliminations upon photodissociation of CH_3CH_2-COCl in the argon matrix at 10 K. The S_0 and S_1 states are degenerate at the C−Cl separation of about 3.2 Å. Before the C−Cl bond is completely broken along the S_1 pathway, the CH_3-CH_2COCl molecule can be reformed, which is followed by the HCl elimination in the ground state. This is the minor channel that is responsible for formation of HCl in the gas phase.

Acknowledgment. This work was supported by grants from the National Natural Science Foundation of China (Grant Nos. 20472011 and 20233020) and from the Major State Basic Research Development Programs (Grant Nos. 2004CB719903 and 2002CB613406).

Supporting Information Available: Structures and energies for all stationary points reported in the present work, as well as the complete refs 20 and 21. These materials are available free of charge via the Internet at http://pubs.acs.org.

References and Notes

(1) Li, H.; Li, Q.; Mao, W.; Zhu, Q.; Kong, F. *J. Chem. Phys.* **1997**, *106*, 5943.
(2) Winter, P. R.; Rowland, B.; Hess, W. P.; Radziszewski, J. F.; Nimlos, M. R.; Ellison, G. B. *J. Phys. Chem. A* **1998**, *102*, 3238.
(3) McCunn, L. R.; Krisch, M. J.; Takematsu, K.; Butler, L. J. *J. Phys. Chem. A* **2004**, *108*, 7889.
(4) Seinfeld, J. H.; Pandis, S. N. *Atmospheric Chemistry and Physics: From Air Pollution to Climate Change*; John Wiley & Sons: New York, 1998.
(5) Vaida, V.; Solomon, S.; Richard, E. C.; Ruhl, E.; Jefferson, A. *Nature* **1989**, *342*, 405.
(6) Mereau, R.; Rayez, M.-T.; Rayez, J.-C.; Caralp, F.; Lesclaux, R. *Phys. Chem. Chem. Phys.* **2001**, *3*, 4712.
(7) Karlsson, H. *J. Mol. Struct*. **1976**, *33*, 227.
(8) Mata, F.; Alonso, J. L. *J. Mol. Struct*. **1979**, *56*, 199.
(9) Frankiss, S. G.; Kynaston, W. *Spectrochim. Acta* **1975**, *31A*, 661.
(10) Dyngeseth, S.; Schei, S. H.; Hagen, K. *J. Mol. Struct*. **1984**, *116*, 257.
(11) Durig, J. R.; McArver, A. Q.; Phan, H. V.; Guirgis, C. A. *J. Phys. Chem.* **1991**, *95*, 539.
(12) Rowland, B.; Hess, W. P. *J. Phys. Chem. A* **1997**, *101*, 8049.
(13) Deshmukh, S.; Myers, J. D.; Xantheas, S. S.; Hess, W. P. *J. Phys. Chem.* **1994**, *98*, 12535.
(14) Durig, J. R.; Li, Y.; Shen, S.; Durig, D. T. *J. Mol. Struct.* **1998**, *449*, 131.
(15) Becke, A. D. *J. Chem. Phys.* **1993**, *98*, 1372. Becke, A. D. *J. Chem. Phys.* **1993**, *98*, 5648.
(16) Lee, C.; Yang, W.; Parr, R. G. *Phys. Rev. B* **1988**, *37*, 785.
(17) Schmidt, M. W.; Gordon, M. S. *Annu. Rev. Phys. Chem.* **1998**, *49*, 233.
(18) Frisch, M. J.; Ragazos, I. N.; Robb, M. A.; Schlegel, H. B. *Chem. Phys. Lett.* **1992**, *189*, 524.; Yamamoto, N.; Vreven, T.; Robb, M. A.; Frisch, M. J.; Schlegel, H. B. *Chem. Phys. Lett*. **1996**, *250*, 373.
(19) Dunning, T. H., Jr. *J. Chem. Phys*. **1989**, *90*, 1007. Woon, D. E.; Dunning, T. H., Jr. *J. Chem. Phys.* **1993**, *98*, 1358. Peterson, K. A.; Woon, D. E.; Dunning, T. H., Jr. *J. Chem. Phys*. **1994**, *100*, 7410.
(20) Frisch, M. J., et al. *Gaussian 98*; Gaussian, Inc.: Pittsburgh, PA, 1998.
(21) MOLPRO is a package of ab initio programs written by Werner, H.-J., et al.
(22) Thompson, D. L. In *Encyclopedia of Computational Chemistry*; Schleyer, P. v. R., Allinger, N. L., Kollman, P. A., Clark, T., Schaefer, H. F., III, Gasteiger, J., Schreiner, P. R., Eds.; Wiley: Chichester, 1998; p 3506.
(23) Bolton, K.; Hase, W. L.; Peshlherbe, G. H. In *Modern Methods for Multidimensional Dynamics Computation in Chemistry*; Thompson, D. L., Ed.; World Scientific: Singapore, 1998; p 143.
(24) Helgaker, T.; Uggerud, E.; Jensen, H. J. A. *Chem. Phys. Lett.* **1990**, *173*, 145.
(25) Millam, J. M.; Bakken, V.; Chen, W.; Hase, W. L.; Schlegel, H. B. *J. Chem. Phys.* **1999**, *111*, 3800.
(26) Sun, L.; Song, K.; Hase, W. L. *Science* **2002**, *296*, 875.
(27) Ammal, S. C.; Yamataka, H.; Aida, A.; Dupuis, M. *Science* **2003**, *299*, 1555.
(28) Hepburn, J. W.; Buss, R. J.; Butler, J. L.; Lee, Y. T. *J. Phys. Chem.* **1983**, *87*, 3638.
(29) Li, X.; Millam, J. M.; Schlegel, H. B. *J. Chem. Phys.* **2001**, *114*, 8897.
(30) King, R. A.; Allen, W. D.; Schaefer, H. F., III. *J. Chem. Phys.* **2000**, *112*, 5585.
(31) Diau, E. W.-G.; Kotting, C.; Zewail, A. H. *ChemPhysChem* **2001**, *2*, 273.
(32) Fang, W.-H.; Liu, R.-Z. *J. Chem. Phys.* **2001**, *115*, 10431.
(33) Chen, X.-B.; Fang, W.-H. *J. Am. Chem. Soc.* **2003**, *125*, 9689.
(34) Eyring, H.; Lin, S. H.; Lin, S. M. *Basic Chemical Kinetics*; Wiley: New York, 1980.
(35) Miller, W. H. *J. Am. Chem. Soc.* **1979**, *101*, 220.
(36) Cossi, M.; Barone, V.; Robb, M. A. *J. Chem. Phys.* **1999**, *111*, 5295.